Chemical Papers (2018) 72:3169–3178
https://doi.org/10.1007/s11696-018-0551-2

ORIGINAL PAPER

Hydrothermal process of synthetic gibbsite and the characteristics of Na in gibbsite crystal

Hui-bin Yang[1] · Feng-qin Liu[2] · Hong-liang Zhao[2] · Rui Wu[3]

Received: 20 February 2018 / Accepted: 4 July 2018 / Published online: 10 July 2018
© Institute of Chemistry, Slovak Academy of Sciences 2018

Abstract
The presence of Na in synthetic gibbsite was studied by several modern testing methods such as X-ray diffraction, scanning electron microscopy, energy-dispersive X-ray spectroscopy and inductively coupled plasma. Results show that Na is located between gibbsite crystals and is not present as sodium aluminosilicate hydrate in synthetic gibbsite. Synthetic gibbsite crystal can be transformed into boehmite under the hydrothermal condition of 210 °C for 60 min. During the reaction process, synthetic gibbsite crystal particles break up into small fragments and form boehmite. During the process, impurities are released and the Na can be removed by washing. Over 90% of Na can be removed during the hydrothermal transformation process. This technology can be applied in the production process of high-purity alumina.

Keywords Sodium · Hydrothermal reaction · Gibbsite · Boehmite · High-purity alumina

Introduction

Gibbsite occurs naturally in gibbsitic bauxite and is usually found alongside goethite, hematite, kaolinite and quartz (Herrmann et al. 2007; Mutakyahwa et al. 2003; Baiocchi 2002). Pure gibbsite or synthetic gibbsite can only be produced in the laboratory or in alumina refineries. Precipitation is the most common method used in the industry to produce synthetic gibbsite from sodium aluminate solution.

Synthetic gibbsite comprises mostly sodium (Na), where the Na is an impurity. Gibbsite sample from alumina refineries contains approximately 1500 ppm Na. Synthetic gibbsite containing various forms of Na can be obtained in the laboratory. According to the synthetic method used, the content of Na fluctuates between 500 and 3000 ppm (Shiwen and Haiyan 2005; Hong and Yangdong 2012).

It is necessary to reduce or control Na impurities in aluminum refineries and other applications during the production process (Guihua et al. 2014; Lanhao 2011). High-purity alumina requires that the impurity content is very low, therefore, as much Na content as possible must be removed so that synthetic gibbsite can be used as a raw material (Dongzhan et al. 2012). The methods used to decrease the content of Na in the synthetic gibbsite production process are widely reported in the literature, but few investigate how the Na come to exist in the gibbsite crystal.

According to the analysis of precipitation process and sodium aluminate solution, there maybe two categories of Na. One is a simple Na component and the other is present as sodium aluminosilicate hydrate.

During the precipitation process, gibbsite crystals have multiple ways of growing such as aggregation of fine crystal particles, single-crystal two-dimensional growing, and two-dimensional nucleation on the surface flaw of the crystal. The crystal growing mode is intricate (Qiusheng et al. 2009; Freij et al. 2004). When precipitation reaction occurs in the sodium aluminate solution the Na is abundant, thus a small amount of Na may be wrapped within the growing crystal particles.

A small amount of SiO_2 is present in industrial sodium aluminate solution which may bring about desilication

✉ Hui-bin Yang
yhuibin@126.com

✉ Feng-qin Liu
zz.sj.lfq@163.com

[1] Hangzhou Yinsheng Enterprise Management Co., Ltd, Hangzhou 310007, China

[2] School of Metallurgical and Ecological Engineering, University of Science and Technology Beijing, Beijing 100083, China

[3] Shandong Drug and Food Vocational College, Zibo 255000, China

reaction that produces sodium aluminosilicate hydrate under some conditions (Fangfang et al. 2016; Xiaolin et al. 2016; Zhengping et al. 2008). The desilication reaction may be influenced by several factors such as Al_2O_3 concentration, SiO_2 concentration, temperature, and standing time (Yifei et al. 2004). The driving force of the desilication reaction rises with the increase in the silica concentration, temperature, and standing time, but declines with an increase in the Al_2O_3 concentration. The mole ratio of alumina vs silica (A/S) is the most important index to measure the stability of sodium aluminate solution. The lower the A/S, the stronger the desilication driving force.

Synthetic gibbsite is generally selected as the raw material to produce high-purity alumina (Wen 2015; Qiaoying et al. 2003). Na enters the solution along during the acid digestion of synthetic gibbsite and can be removed easily. However, during the alkaline process, the Na is the major impurity in the synthetic gibbsite and is hard to remove. The process of removing Na and other impurities is required for the production of high-purity alumina. Several raw materials can be used to produce high-purity alumina and production methods are numerous. Liu Jianliang selected high-purity aluminum as a raw material and used rapid cooling atomization to produce high-purity alumina powder (Jianliang 2005). The alcohol–aluminum hydrolysis process was used by Ying (2015) to produce 4N (99.99%) class high-purity alumina.

$Al(OH)_3$ is typical synthetic gibbsite which has good reaction activity and transforms into different products during the hydrothermal process. Jun (2009) studied the hydrothermal law of $Al(OH)_3$ in different kinds of solutions. Part of gibbsite transformed into boehmite after 24 h of hydrothermal treatment in water at 140 °C. The gibbsite crystal particles break from the block and form a flaky structure. Under the same reaction conditions, the hydrothermal product is boehmite when isopropanol and sodium carbonate solution is used, and the crystal produced is a three-dimensional interleaved structure consisting of nano-flakes. When the reaction medium occurs in a urea solution, the hydrothermal product is ammonium aluminum carbonate hydroxide and the crystal is a micro-sphere consisting of wattle. Yanming et al. (2003) studied the hydrothermal reaction of $Al(OH)_3$ at 340 °C. They observed that the hydrothermal product suffered a 50% loss on ignition (LOI) when the solution contained certain additives.

In this work, the characteristics of Na in synthetic gibbsite were studied for various aspects of the crystal transformation process under hydrothermal conditions. Results provide support for the production process of high-purity alumina.

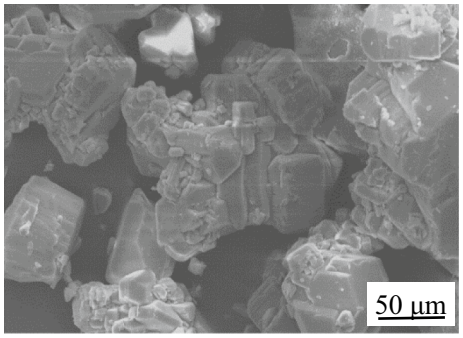

Fig. 1 SEM image of sample

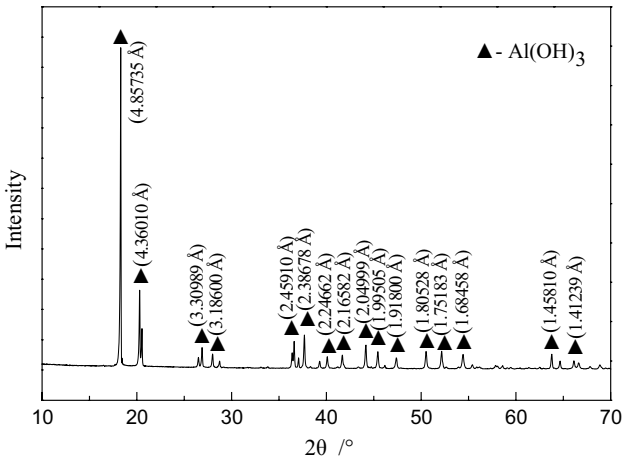

Fig. 2 XRD pattern of sample

Material and test methods

$Al(OH)_3$ was selected as the raw material to produce high-purity alumina. The mid-particle size of the sample as analyzed by a laser particle analyzer is 115.38 μm. The SEM and XRD of the sample also were analyzed and the results are shown in Figs. 1 and 2, respectively.

The synthetic gibbsite is the product of carbonization precipitation. The SEM image shows that the crystal particle of the sample clearly shows the characteristics of polymerization.

The XRD pattern (Fig. 2) shows that the sample is pure gibbsite and no other mineral was found to be present.

In this study, the test method employed was high-pressure hydrothermal treatment and the medium solution was deionized water. The mass ratio of the water in comparison to the sample was set at 10 in the solution. The hydrothermal reaction performed in the homogeneous reactor provided high-temperature- and high-pressure conditions. All the reaction times were set to 60 min and the temperature

varied from 160 to 220 °C. After the reaction, the slurry was filtered, the resulting filter cake was then washed and dried in a drying oven. Then the test products were analyzed by several methods such as XRD, SEM, EDS, and ICP. Finally, the characteristics of Na in the synthetic gibbsite and the behavior of Na during the hydrothermal process were discussed according to the test results.

Analysis instruments and methods

X-ray diffraction (XRD) of the samples were analysed by a D8ADVANCE X-ray diffraction with a Cu target cathode. The λ was 0.15418 nm. The voltage was 30 kV, the tube current was 15 mA, the scanning angle varied from 10° to 70°, and the scanning speed was 4°/min with the step size 0.02°. Scanning electron microscopy (SEM) observations of the samples were performed on a S4800 cold field emission scanning electron microscope equipped with an energy-dispersive X-ray spectroscopy (EDS) apparatus. The resolution ratio was 1.00 nm (15 kV), and the acceleration voltage was 10 kV. Trace element detection was performed on a 7700 × inductively coupled plasma (ICP) and the test accuracy was 0.5 ppb.

A homogeneous reactor was selected to perform the hydrothermal reaction, which was equipped with six independent reactors and the volume of the single reactor was 150 ml. The temperature of the reactor varied from 25 to 300 °C. Other universal test equipment used, included a mechanical stirrer and circulating water multi-purpose vacuum pump.

Results and discussion

Phase transformation law of synthetic gibbsite

Hydrothermal reaction of synthetic gibbsite was performed in a homogeneous reactor at 160–220 °C. The step size of the temperature rise was 10 °C and the reaction time was 60 min. XRD patterns of the test products were analysed and put into one figure in order to study the phase changes. The XRD patterns are shown in Fig. 3.

As shown in Fig. 3, the mineral structure of the sample did not change below 190 °C. Tiny changes of the XRD pattern occurs at 190 °C which indicated that phase react had begun. The XRD pattern shows obvious change at 200 °C, part of the boehmite has formed, but gibbsite is also present in the product which comprised a mixture of boehmite and gibbsite. When the hydrothermal temperature reached 210 °C, the diffraction peaks of gibbsite disappeared and boehmite became the only component in the product. The XRD pattern of the sample heated to 220 °C was the same that was obtained at 210 °C which indicates that the reaction

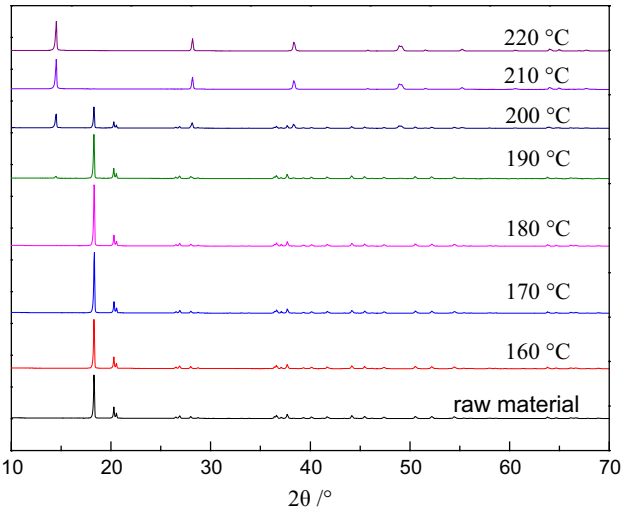

Fig. 3 XRD patterns of whole test samples

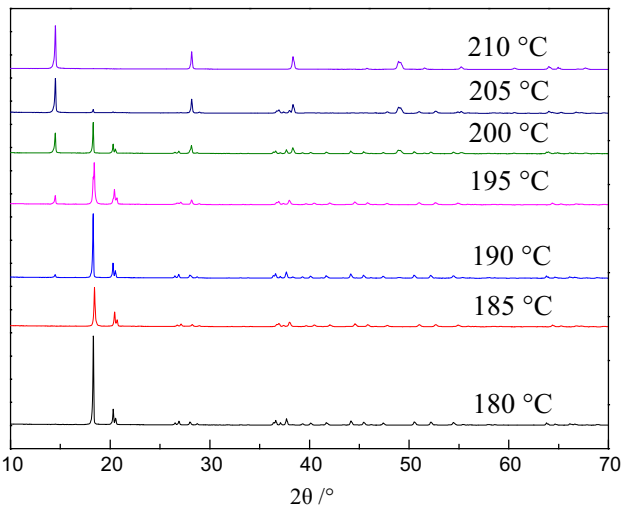

Fig. 4 XRD patterns of test samples (step size 5 °C)

was completed at 210 °C and the reaction product remained constant above 210 °C.

To show the reaction temperature more accurately, the step size of the temperature rise was reduced to 5 °C and the reaction time was 60 min. The XRD patterns of test samples are shown in Fig. 4.

As shown in Fig. 4, the changes have not begun at 185 °C. Obvious changes could be found at 195 °C. When the temperature was 205 °C, the XRD pattern showed several tiny gibbsite diffraction peaks which indicated that the reaction had not finished. At 210 °C, the gibbsite diffraction peaks disappeared completely in the XRD pattern.

At 200 °C, the product was more complex and needed to be analysed carefully. The XRD pattern of the product is shown in Fig. 5.

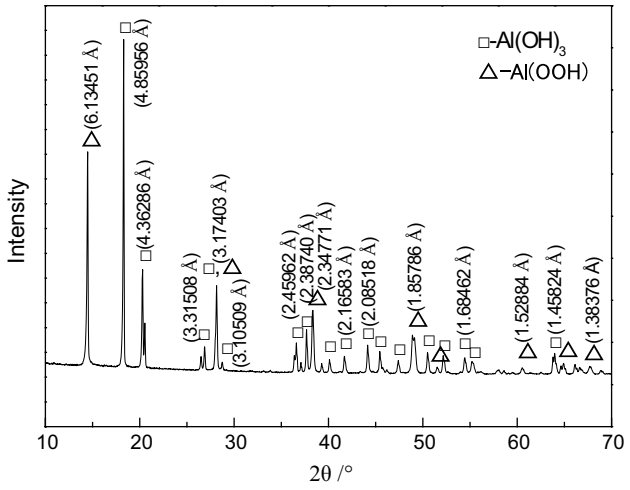

Fig. 5 XRD pattern at 200 °C

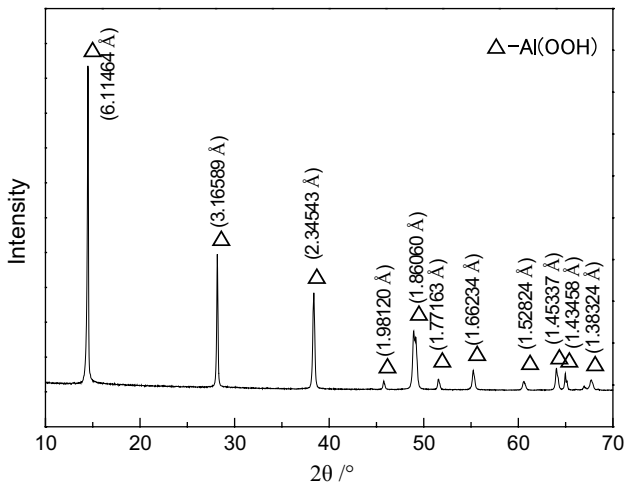

Fig. 6 XRD pattern of 210 °C

In the standard XRD pattern card, the three main diffraction peaks of the boehmite are located at 6.11000, 3.16400, and 2.34600 Å with the diffraction intensities at 100, 65, and 55%, respectively. As shown in Fig. 5, the three main diffraction peaks of boehmite have already appeared in the product under the reaction condition of 200 °C for 60 min which indicates that boehmite has been produced. At the same time, the diffraction peaks of gibbsite were also present in the XRD pattern of sample produced at 200 °C which indicated only part of the gibbsite transformed into boehmite and the reaction had not completed.

As shown in Fig. 3, the XRD pattern stabilized at 210 °C which indicates the hydrothermal reaction was fully completed in 60 min at this temperature. The XRD pattern of the 210 °C product is shown in Fig. 6.

As shown in Fig. 6, boehmite was the unique mineral in the product which indicates the hydrothermal reaction had finished and that the gibbsite had successfully and completely transformed into boehmite at 210 °C in 60 min. The base line of the XRD pattern was flat and no impure peak appeared which indicates the boehmite was well crystallized and had good crystallinity.

The results of the hydrothermal test showed that the crystal of the gibbsite could transform into boehmite completely at about 210 °C for 60 min. The reaction began at 190 °C but there was far less boehmite in the test product. The test product was a mixture of boehmite and gibbsite in samples produced at 200 °C for 60 min. When the reaction temperature reached 210 °C or more, the gibbsite transformed into boehmite completely in 60 min and the only reaction product is boehmite.

Microcrystal morphology of the test product

Internal stress appeared in the crystal particles while the mineral was undergoing crystal transformation. The stress damaged the original structure of the crystal particles which could be observed in the micromorphology of the samples. The SEM images of test samples are shown in Fig. 7.

As shown in Fig. 7, the crystal particle surface of the synthetic gibbsite shows no change when the hydrothermal temperature was below 180 °C (Fig. 7a, b). When the temperature was 190 °C (Fig. 7c), the edge of the particle became sharper than before, and fine particles were more obvious. The change indicates that gibbsite has begun the crystal transformation at this temperature, but interestingly this change was not clear in the corresponding XRD pattern (Fig. 3) which points to the fact that 190 °C was the critical point and the transformation had not really started yet. When the temperature was 200 °C (Fig. 7d), fine flaky or flaky-layered particles with sharp edges began to appear. The sample consisted of flaky particles and big blocky particles. Combined with the XRD test results (Fig. 5), it can be concluded that the big blocky particles were gibbsite particles and the fine flaky particles were boehmite. When the temperature was 210 °C (Fig. 7e), major fragmentation of the big blocky particles occurred and the sharp edges of the fine particles were more noticeable. At 220 °C (Fig. 7f), almost all particles were present as fine flaky particles with sharp edges and no big blocky particles were found. As shown in Figs. 3 and 6, the reaction product comprised boehmite when the temperature was above 210 °C.

The crystal morphology of the fine flaky particles was related to the crystal structure of gibbsite. Research results show that the inner crystal structure of gibbsite was composed of flaky-layered and numerous flakes superimposed on one another forming spherical crystal granules (Huibin 2016). This characteristic is shown in Fig. 6a, where the

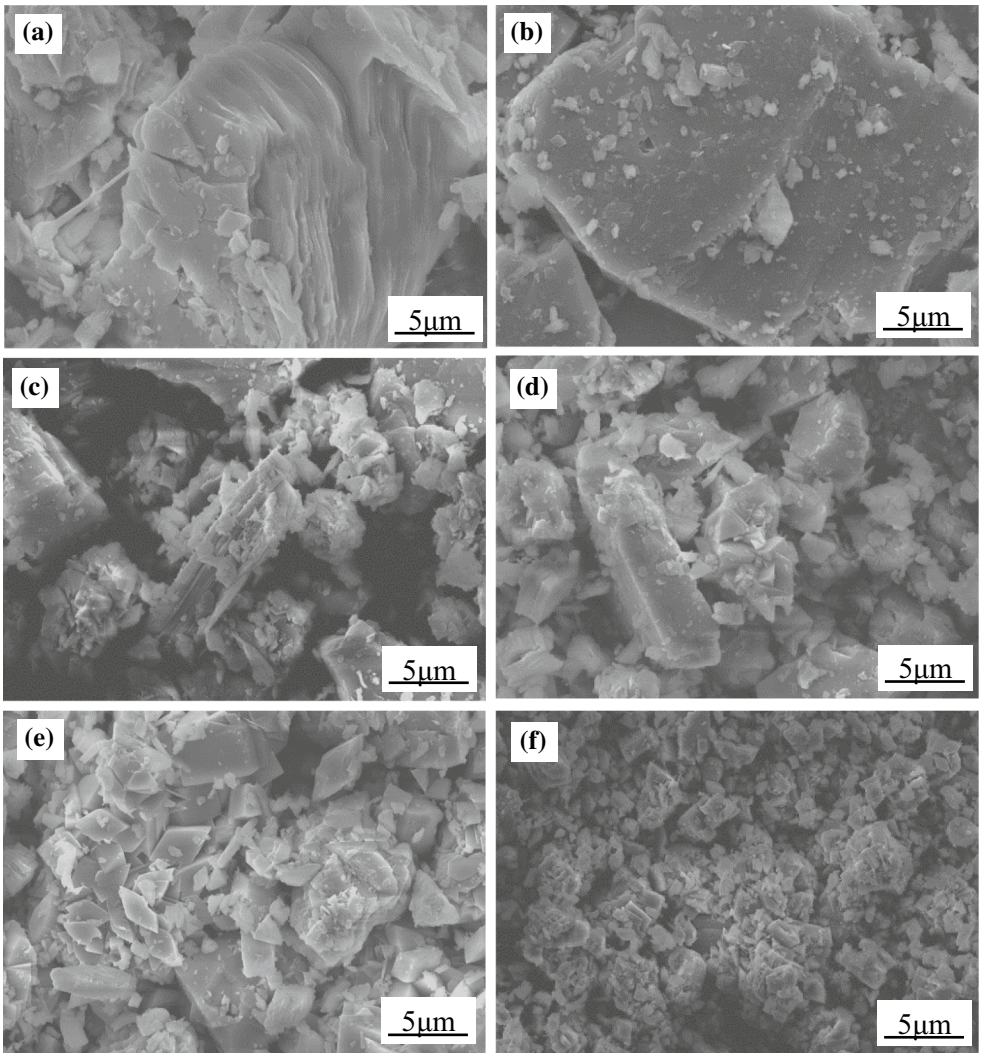

Fig. 7 SEM images of test samples (**a** 160 °C; **b** 180 °C; **c** 190 °C; **d** 200 °C; **e** 210 °C; **f** 220 °C)

particle edge of the gibbsite demonstrated obvious flaky-layered structure. In hydrothermal reaction process, the crystal particle was broken apart but no change occurred in the flaky shape of the fine particle because gibbsite converted into boehmite and the lattice recombined, making the crystal particle edge of boehmite sharp. This hydrothermal reaction process could be used to grind the gibbsite crystal particles, a method that is obviously very different from the traditional machine-grinding process.

Analysis of the characteristics of Na element

Na element occurs as an impurity in synthetic gibbsite. We presumed that there are two categories Na, one is present as sodium aluminosilicate hydrate another is trapped between gibbsite crystals. Both of them demand greater and more careful discussion.

A small amount of silica is to be found in industrial sodium aluminate solution, so the solution may undergo desilication reaction under some conditions. The desilication product (DSP) is sodium aluminosilicate hydrate. The equation of desilication reaction may be represented as Eq. (1)

$$\begin{aligned} &Na_2O \cdot Al_2O_3 + Na_2O \cdot SiO_2 + aq \\ &\quad \rightarrow Na_2O \cdot Al_2O_3 \cdot 1.8SiO_2 \cdot 2.4H_2O + aq \end{aligned} \tag{1}$$

If the solution undergoes desilication reaction according to Eq. (1), the DSP would appear in the synthetic gibbsite and the Na would present in DSP.

The SEM images of pure DSP are shown in Fig. 8. The sample of DSP was produced in the laboratory.

As shown in Fig. 8, the DSP crystal particle looks like a ball of yarn. A number of small balls combine to form a large irregular-shaped DSP crystal particle. There are distinct differences between the crystal morphology and the

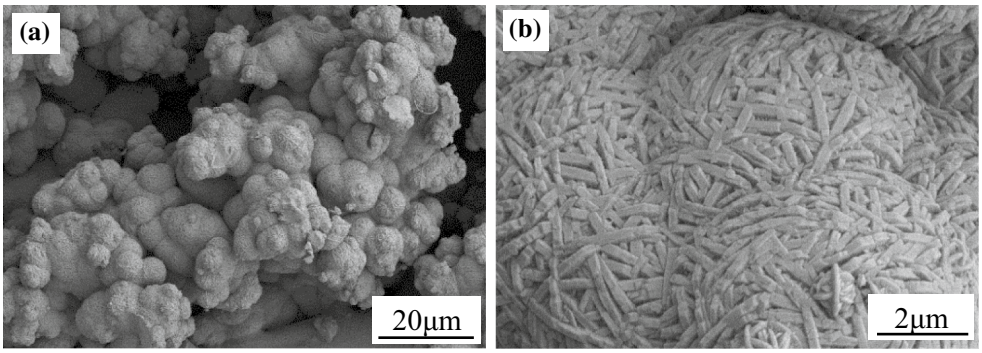

Fig. 8 SEM images of DSP (**a** crystal particles; **b** surface of crystal)

flaky-layered gibbsite structure, a difference that allows for easy detection of DSP by SEM and EDS (Huibin 2016; Huibin et al. 2015).

The SEM and EDS of most test samples were analyzed to find DSP. All analysis was focused on the fine particles with unusual morphology. The results of the analysis are shown in Figs. 9, 10, 11, 12, 13, and 14.

As shown in the results of SEM and EDS, the main element components of all the fine particles were O and Al. No Na or Si existed in the particles which means no DSP is presented in the particles. Except for the EDS test results of Figs. 9, 10, 11, 12, 13, and 14, a large number of particles were analyzed too, and no DSP were found. This indicated that no DSP existed in the synthetic gibbsite particles.

Actually, the SiO_2 concentration appears lower in the process of industrial production and the mole ratio of alumina vs silica (A/S) is higher in the refined sodium aluminate solution. The desilication reaction can happen only when A/S is lower. The A/S of industrial sodium aluminate solution is about 200–1000 and the precipitation mother liquid is approximately 50–100. In this kind of solution, the concentration of SiO_2 has not yet reached the metastable equilibrium concentration and normally the desilication reaction does not take place.

Agglomeration and growth are two ways in which crystal particles of $Al(OH)_3$ develop from sodium aluminate solution. According to the regional refining theory, impurities cannot enter the crystal structure of $Al(OH)_3$. Nevertheless, cavities may present in the agglomeration process of multiple small $Al(OH)_3$ crystals. The cavities would not be empty but filled with solution. There is plenty of Na in sodium aluminate solution, so the Na can be present in the cavity solution and become trapped within gibbsite crystal particles. The Na would be released when the gibbsite crystal breaks up.

Variation of Na content in hydrothermal process

The crystal transformation during the hydrothermal process leads to changes of the Na element content. ICP was used to analyze the Na content of the samples. The hydrothermal

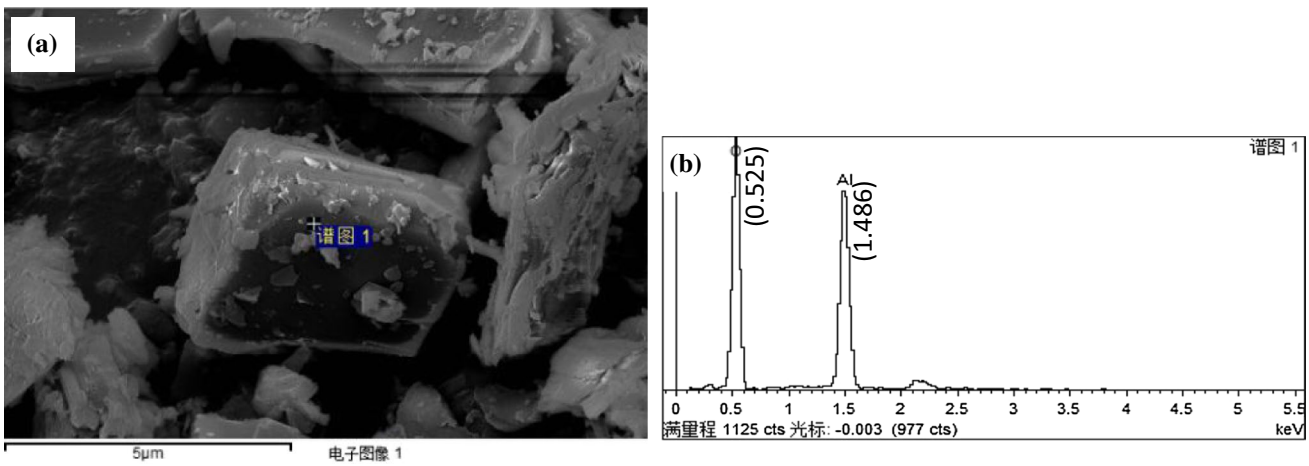

Fig. 9 SEM image (**a**) and EDS pattern (**b**) of raw material

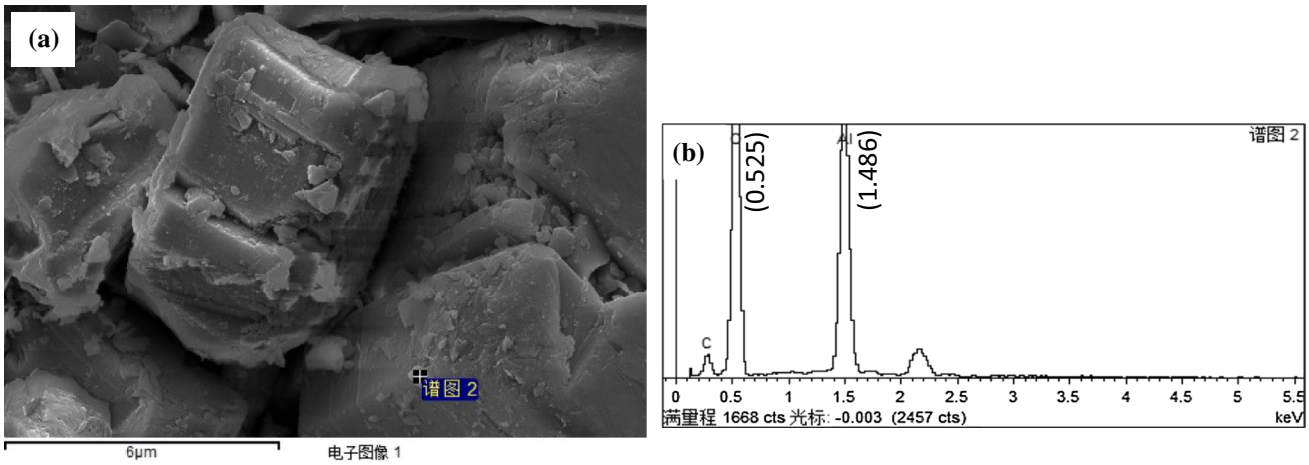

Fig. 10 SEM image (**a**) and EDS pattern (**b**) of 160 °C test product

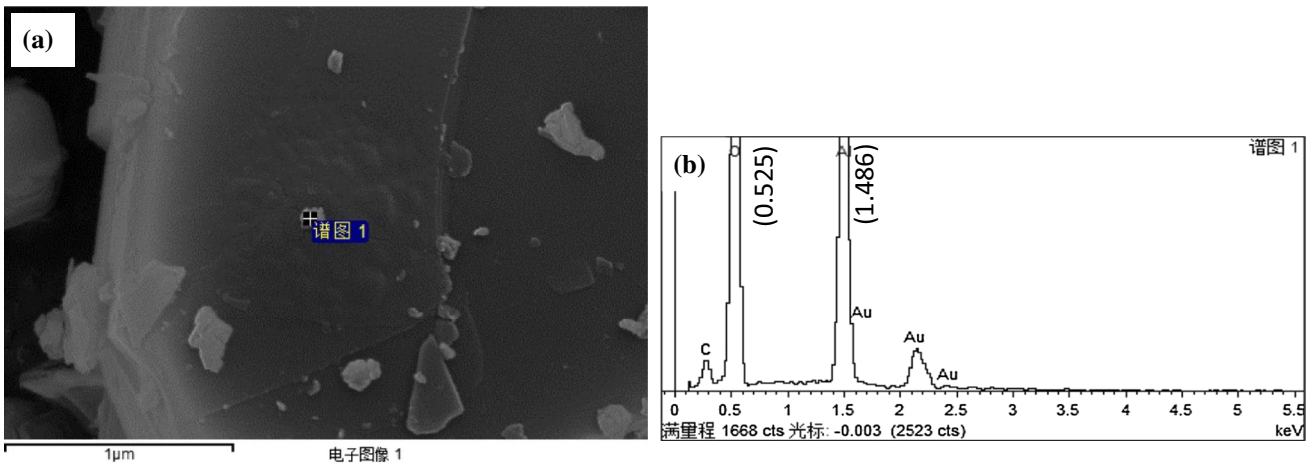

Fig. 11 SEM image (**a**) and EDS pattern (**b**) of 170 °C test product

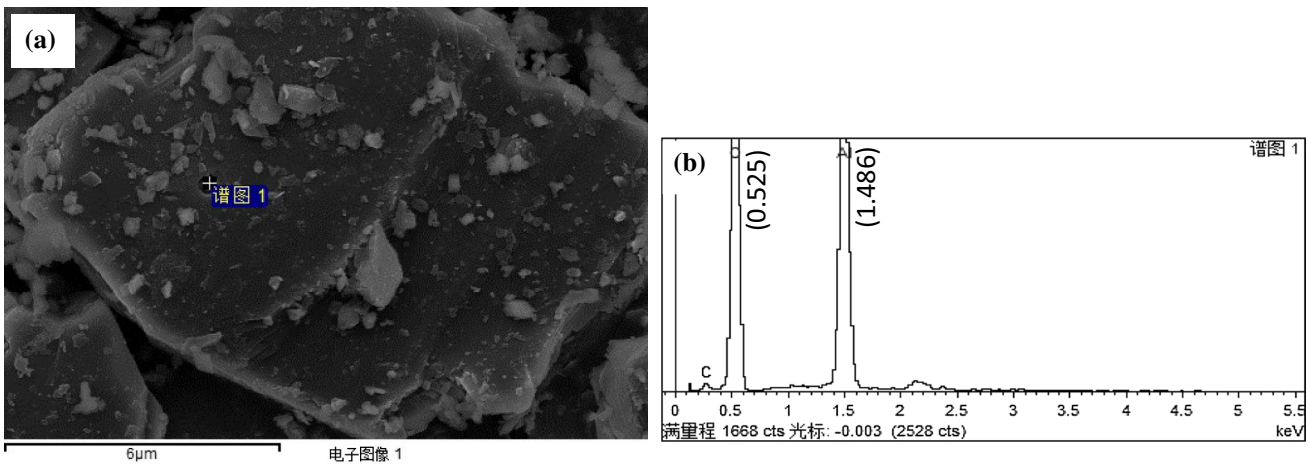

Fig. 12 SEM image (**a**) and EDS pattern (**b**) of 180 °C test product

temperature varied from 160 to 220 °C and analysis results of test samples are shown in Table 1.

As shown in Table 1, the content of Na in the samples gradually decreased as the hydrothermal temperature increased. The hydrothermal reaction was not obvious before 190 °C, so the corresponding decrease in Na content was not remarkable. The reaction began at 200 °C when the Na content began to decrease, but the Na content of the samples was still high because the samples consisted of gibbsite and boehmite at this temperature and the crystal particles had not yet completely disintegrated. When the temperature reached 210 °C, all the gibbsite transformed into boehmite in 60 min and the crystal particles completely shattered resulting in a major decrease in the Na content. When the temperature reached 220 °C, the content of Na was 36.62 ppm which showed a reduction of 90.14% compared with the starting material. Si, Fe, and Ca were the by-products of synthetic gibbsite and their contents were analysed. The contents of the by-products (Si, Fe, and Ca) of synthetic gibbsite were lower which means the test errors were relatively higher. The results show that the contents of those elements only slightly decreased and the change law was not so obvious.

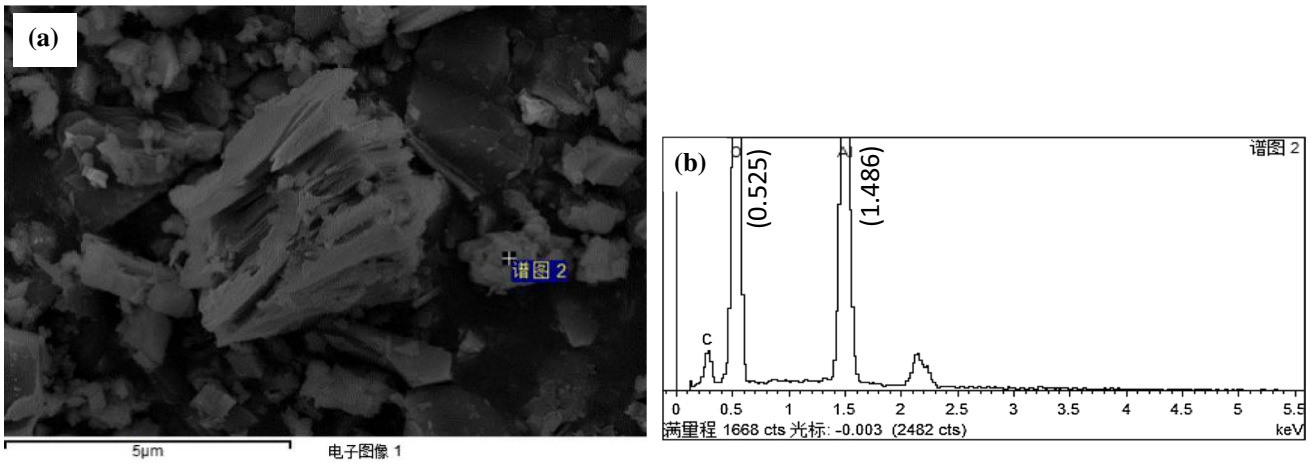

Fig. 13 SEM image (**a**) and EDS pattern (**b**) of 190 °C test product

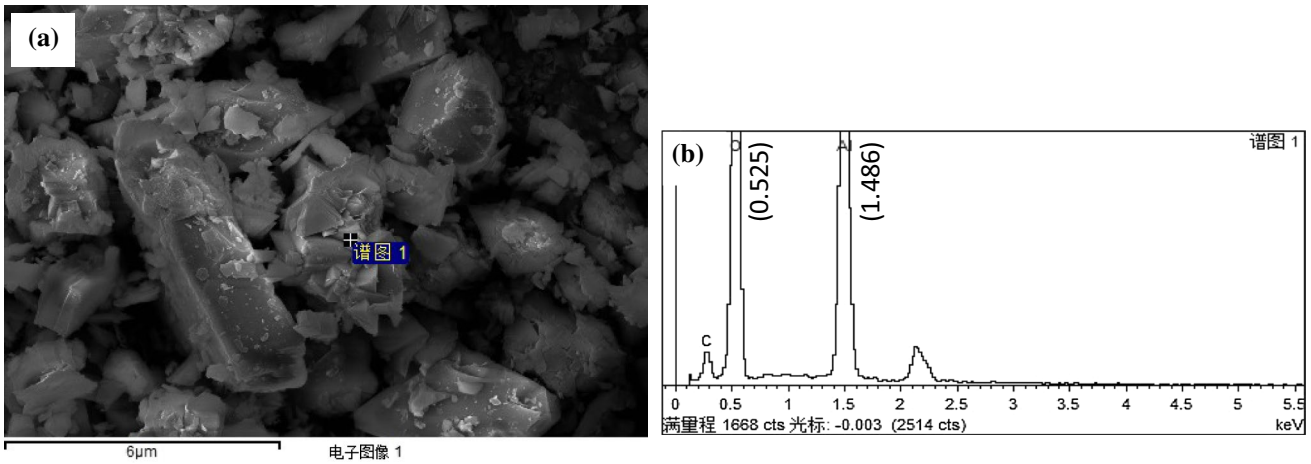

Fig. 14 SEM image (**a**) and EDS pattern (**b**) of 200 °C test product

Table 1 Na content of test samples (ppm)

Sample	Raw material	Hydrothermal temperature/ °C						
		160	170	180	190	200	210	220
Na content of samples	753.9	692.28	637.80	633.25	568.62	488.02	42.41	36.62

The test results of ICP also indicated that the Na occurred between gibbsite crystals. Agglomeration was one of the main ways by which gibbsite crystal developed during the precipitation process. The Na was sandwiched between the crystals during the precipitation process and produced a higher Na content in synthetic gibbsite. When crystal transition occurred during the hydrothermal process, the gibbsite crystal particles shattered due to internal stress and Na was released into the solution. Therefore, with the increase of crystal transformation, the content of Na in the sample was continually reduced. This technology and reaction mechanism could be used for the production of high-purity alumina. The Na can be removed by employing hydrothermal reaction when synthetic gibbsite was selected as the raw material.

Conclusions

Experiments conducted here have shown that Na occurs between the gibbsite crystals in synthetic gibbsite. No sodium aluminosilicate hydrate crystal was found in the synthetic gibbsite crystal particles.

Synthetic gibbsite underwent the hydrothermal reaction and transformed into boehmite in water under the conditions of 210 °C for 60 min. During the hydrothermal reaction process, the gibbsite crystals splintered into small flaky particles and most particles were below 5 μm in size. Fragmentation of crystal particles allows for the release of intergranular Na more than 90% of which can be removed during the hydrothermal reaction process.

The test results and reaction mechanism could be used to produce high-purity alumina, a technique that can remove most of the Na impurities without creating any other impurities and offer a better method of removing impurities. But this hydrothermal process is just one part of the high-purity alumina production process. This technology only can decrease Na to less than 100 ppm, then other technics are needed to reduce Na until it can reach the quality requirements of high-purity alumina.

References

Baiocchi L (2002) Distribution and dynamics of gibbsite and kaolinite in an oxisol of Serra do Mar. southeastern Brazil. Geoderma 106(1–2):83–100. https://doi.org/10.1016/S0016-7061(01)00117-3

Dongzhan H, Zhonglin Y, Jianli W (2012) High purity alumina production technology and application research progress. Inorg Chem Ind 44(9):1–4. https://doi.org/10.3969/j.issn.1006-4990.2012.09.001 **(in chinese)**

Fangfang C, Yifei Z, Xiaoduo J, Shaotao C, Shaowei Y, Yi Z (2016) Structure transformation of sodium aluminosilicates as desilication agents in the desilication of highly alkaline sodium aluminate solution containing silica. Microporous Mesoporous Mater 235(11):224–232. https://doi.org/10.1016/j.micromeso.2016.08.011

Freij SJ, Parkinson GM, Reyhani MM (2004) Direct observation of the growth of gibbsite crystals by atomic force microscopy. J Cryst Growth 260(1–2):232–242. https://doi.org/10.1016/j.jcrysgro.2003.08.064

Guihua L, Peng W, Tiangui Q, Xiaobin L, Lu T, Qiusheng Z, Zhihong P (2014) Variation of soda content in fine alumina trihydrate by seeded precipitation. Trans Nonferr Metals Soc China 24(1):243–249. https://doi.org/10.1016/S1003-6326(14)63053-3

Herrmann L, Anongrak N, Zarei M, Schuler U, Spohrer K (2007) Factors and processes of gibbsite formation in Northern Thailand. Catena 71(2):279–291. https://doi.org/10.1016/j.catena.2007.01.007

Hong L, Yangdong N (2012) Measures to reduce the content of sodium oxide in aluminum hydroxide. Energy Sav Non-Ferr Metall 28(4):20–22. https://doi.org/10.3969/j.issn.1008-5122.2012.04.006 **(in chinese)**

Huibin Y (2016) The dissolution process and kinetics of high iron gibbsitic bauxite under atmospheric pressure. Ph.D. thesis, Northeastern University, Shenyang. **(in chinese)**

Huibin Y, Xiaolin P, Haiyan Y, Ganfeng T, Junmin S (2015) Dissolution kinetics and mechanism of gibbsitic bauxite and pure gibbsite in sodium hydroxide solution under atmospheric pressure. Trans Nonferr Metals Soc China 25(12):4151–4159. https://doi.org/10.1016/S1003-6326(15)64065-1

Jianliang L (2005) The study of aluminum high produce high pure alumina by hydrolysis process. Ph.D. thesis, Kunming University of Science and Technology, Kunming. **(in chinese)**

Jun S (2009) Modification study of the aluminum hydroxide microstructure by hydrothermal treatment. M.D. thesis, Dalian Jiaotong University, Dalian. **(in chinese)**

Lanhao C (2011) Study on preparation process of low sodium hydroxide. M.D. thesis, Xi'an University of Architecture and Technology, xi'an. **(in chinese)**

Mutakyahwa MKD, Ikingura JR, Mruma AH (2003) Geology and geochemistry of bauxite deposits in Lushoto District, Usambara Mountains, Tanzania. J Afr Earth Sci 36(4):357–369. https://doi.org/10.1016/S0899-5362(03)00042-3

Qiaoying C, Xinwei W, Yongmin B (2003) High pure alumina micropowders prepared with neutral method. China Powder Sci Technol 9(4):16–18. https://doi.org/10.3969/j.issn.1008-5548.2003.04.006 **(in chinese)**

Qiusheng Z, Dianjun P, Zhihong P, Guihua L, Xiaobin L (2009) Agglomeration of gibbsite particles from carbonation process of sodium aluminate solution. Hydrometallurgy 99(3–4):163–169. https://doi.org/10.1016/j.hydromet.2009.07.015

Shiwen B, Haiyan Y (2005) Alumina production technology. Metallurgical Industry Press, Beijing **(in chinese)**

Wen L (2015) $Al(OH)_3$ produce high purity Al_2O_3 and purification technology research. M.D. thesis, Guizhou Normal University, Guiyang. **(in chinese)**

Xiaolin P, Haiyan Y, Ganfeng T, Shiwen B (2016) Effects of precipitation activity of desilication products (DSPs) on stability of sodium aluminate solution. Hydrometallurgy 165(12):261–269. https://doi.org/10.1016/j.hydromet.2016.01.034

Yanming G, Pengyuan Z, Jianfeng C (2003) Hydrothermal synthesis high efficient ultra-fine aluminum hydroxide flame retardant. Inorg Chem Ind 35(2):26–28. https://doi.org/10.3969/j.issn.1006-4990.2003.02.009 **(in chinese)**

Yifei Z, Shili Z, Yi Z (2004) Stability of the supersaturated silica in sodium aluminate solution. J Chem Ind 55(5):695–698. https://doi.org/10.3321/j.issn:0438-1157.2004.05.003 **(in chinese)**

Ying Z (2015) Laboratory research of producing high pure alumina by Alcohol aluminum hydrolysis process. M.D. thesis, Guizhou University, Guiyang. **(in chinese)**

Zhengping W, Zhoulan Y, Qiyuan C (2008) Influence and interaction mechanism of silicon-containing impurities on the precipitation of sodium aluminate solution process. Chin J Nonferr Metals 18(12):2275–2283. https://doi.org/10.3321/j.issn:1004-0609.2008.12.024 **(in chinese)**